HHS Public Access

Author manuscript

Ophthalmology. Author manuscript; available in PMC 2021 August 01.

Published in final edited form as:

Ophthalmology. 2020 August ; 127(8): 1097–1104. doi:10.1016/j.ophtha.2020.02.024.

Photovoltaic Restoration of Central Vision in Atrophic Age-Related Macular Degeneration

D. Palanker, PhD[1], **Y. Le Mer, MD**[2], **Saddek Mohand-Said, MD**[3], **MMK Muqit, PhD FRCOphth**[4,5], **J.A. Sahel, MD**[2,3,6]

[1]Department of Ophthalmology and Hansen Experimental Physics Laboratory, Stanford University, CA;

[2]Department of Ophthalmology, Fondation Ophtalmologique A. de Rothschild, Paris, France;

[3]Clinical Investigation Center, Quinze-Vingts National Eye Hospital, Paris, France;

[4]Vitreoretinal Service, Moorfields Eye Hospital, London, UK;

[5]Institute of Ophthalmology, University College London, UK;

[6]Department of Ophthalmology, University of Pittsburgh School of Medicine, Pittsburgh, PA.

Abstract

Objective: Loss of photoreceptors in atrophic age-related macular degeneration results in severe visual impairment, although some peripheral vision is retained. To restore central vision without compromising the residual peripheral field, we developed a wireless photovoltaic retinal implant (PRIMA), in which pixels convert images projected from video glasses using near-infrared light, into electric current to stimulate the nearby inner retinal neurons.

Design: We carried out a first in human clinical trial to test the safety and efficacy of the prosthesis in patients with geographic atrophy. (Clinicaltrials.gov NCT03333954)

Subjects: Five patients with geographic atrophy zone of at least 3 optic disc diameters, no foveal light perception and best corrected visual acuity of 20/400 to 20/1000 in the worse-seeing “study” eye.

Methods: The 2 mm-wide, 30 μm-thick chip, containing 378 pixels (each of 100 μm in diameter), was implanted subretinally in the area of atrophy (absolute scotoma).

Address for reprints: Daniel Palanker, 452 Lomita Mall, Stanford, CA 94305.

Preliminary results of this study were presented at the American Academy of Ophthalmology Annual Meeting in October 2018, ARVO in May 2019, and EURETINA in September 2019.

Conflict of Interest: DP’s patents owned by Stanford University are licensed to Pixium Vision. DP, YLM, SMS, and MMKM are consultants to Pixium Vision. JAS discloses founding shares and past consulting for Pixium Vision.

Main Outcome Measures: Anatomical outcomes were assessed with fundus photography and optical coherence tomography up to 12 months follow-up. Prosthetic vision was assessed by mapping light perception, bar orientation, letter recognition, and Landolt C acuity.

Results: In all patients, the prosthesis was successfully implanted under the macula, although in two patients in unintended locations: in one subject - intra-choroidal, and in another - off- center by 2mm. All five could perceive white-yellow prosthetic visual patterns with adjustable brightness in the previous scotomata. The three with optimal placement of the implant demonstrated prosthetic acuity of 20/460 to 20/550, and one with the off-center implant - 20/800. Residual natural acuity did not decrease after implantation in any patient.

Conclusions: Implantation of PRIMA did not decrease the residual natural acuity, and it restored visual sensitivity in the former scotoma in each of the 5 patients. In 3 patients with the proper placement of the chip, prosthetic visual acuity was only 10–30% below the level expected from the pixel pitch (20/420). Therefore, the use of optical or electronic magnification in the glasses as well as smaller pixels in future implants may improve visual acuity even further.

Precis:

Wireless photovoltaic array implanted subretinally in the geographic atrophy and activated via video glasses provides monochromatic central vision with resolution close to a single pixel size, without decreasing the residual eccentric acuity.

Introduction

Age-related macular degeneration (AMD) is a leading cause of irreversible vision loss, affecting over 8.7% of the population worldwide; the number of affected persons is projected to reach 196 million by 2020[1]. Advanced forms of AMD (neovascularization and geographic atrophy) are associated with severe visual impairment, and their prevalence dramatically increases with age: from 1.5% in the US population above 40 years to more than 15% in the population older than 80[2].

Geographic atrophy, which occurs at an advanced stage of the disease, results in gradual loss of photoreceptors in the central macula (which is responsible for high-resolution vision), and severely impairs reading and face recognition. Low-resolution peripheral vision is retained in this condition, necessitating the use of eccentric fixation. Therefore, the goal of any treatment strategy should be to provide functional central vision without jeopardizing the surrounding retina.

While photoreceptors in retinal degeneration are lost, the inner retinal neurons survive to a large extent[3–5]. Electronic retinal prostheses are designed to reintroduce visual information into the degenerate retina by electrical stimulation of the remaining neurons. Current strategies involve placing electrode arrays either subretinally, to stimulate the first layer of neurons above the photoreceptor cells (mainly bipolar cells in the inner nuclear layer (INL)[6–8]), or epiretinally, to target the retinal ganglion cells.[9,10] The epiretinal implant (ARGUS II, Second Sight Inc., Sylmar, California, USA) currently approved for patients blinded by inherited retinal degeneration (retinitis pigmentosa, RP) has 60 electrodes (200 μm in diameter, 575 μm pitch)[11], which are relatively distant (on average, approximately 180

μm) from the target retinal ganglion cells (RGC)[12]. Patients using this system have been reported to have low visual acuity, of 20/1260 or worse.[13] In addition to activation of proximal neurons, this implant stimulates the axons of remote RGCs passing underneath the electrodes, causing distorted visual percepts[14].

Preclinical studies in rodents demonstrated that stimulation of bipolar cells via subretinal implants results in a network-mediated retinal response, which preserves many features of normal vision: flicker fusion at high frequencies (>20 Hz)[15,16] and adaptation to static images[17], "on" and "off" responses to increments and decrements in light with antagonistic center-surround organization[18], and non-linear summation of the inputs from bipolar cells into ganglion cells' receptive fields (so-called sub-units)[16], essential for high spatial resolution.

A subretinal implant Alpha IMS/AMS (Retina Implant AG, Reutlingen, Germany) having up to 1600 pixels, each of 70 μm in width, was tested in patients blinded by RP. Out of 44 trials participants, visual acuity using Landolt C was measurable in 6 patients, ranging from 20/2000 to 20/546 (2 patients)[19,20]. None of the trials' participants achieved an acuity approaching the theoretical limit of resolution of the pixel array, approximately 20/280. This could be due to the monopolar design of this implant, in which active electrodes share a common remote return electrode, an arrangement that may result in strong "cross-talk" between neighboring electrodes and thus limit spatial contrast[21]. It is also possible that the highly remodeled retinal neural network in advanced stages of RP[22] degrades the attainable prosthetic acuity in such patients.

Both these implants are powered via trans-scleral cable inserted in complex surgical procedures associated with postoperative complications[13,19], which may affect residual peripheral vision – an especially important concern for patients with AMD.

PRIMA system

We developed a wireless prosthesis in which photovoltaic pixels directly convert projected light patterns into local electric current[16,23]. It is 2 mm in width (corresponding to about 7 degrees of the visual angle in a human eye), 30 μm in thickness, with 378 pixels, each of which is 100 μm in diameter (PRIMA, Pixium Vision; Figure 1). Images captured by the camera are processed and projected onto the retina from video glasses using near-infrared (NIR, 880 nm) light to avoid photophobic and phototoxic effects of bright illumination[24]. Current flowing through the retina between the local active and return electrodes stimulates the nearby inner retinal neurons[23], which then pass the responses to ganglion cells, thereby harnessing some of the residual retinal signal processing[16,25,26]. To avoid irreversible electrochemical reactions at the electrode–electrolyte interface, stimulation is charge-balanced, and hence it is pulsed with alternating polarity[27]. For continuous perception under pulsed illumination, we apply sufficiently high frequencies to enable flicker fusion. Preclinical studies in rodents demonstrated retinal adaptation to frequencies exceeding 20 Hz under network-mediated stimulation[16,28]. Localization of the electric field is achieved by providing active and return electrodes in each pixel[16]. In preclinical testing in rodents, such photovoltaic arrays with pixels of 75 μm and 55 μm in width provided grating visual acuity (alternating light and dark stripes) matching the pixel density[16,28]. Preclinical testing of the

PRIMA implants having 100 μm pixels in non-human primates demonstrated similar stimulation thresholds to those observed in rodents and perceptual responses (saccadic movement) down to a single pixel activation[29].

Methods

Patients

The aim of this first-in-human feasibility study of the PRIMA implant (NCT03333954) was to test safety and functionality of this device in 5 patients with AMD. The study adhered to the Declaration of Helsinki and received the ethics committee approval from the Comité de Protection des Personnes Ile de France II and by the Agence Nationale de Sécurité du Médicament et des Produits de Santé. Study participants were above 60 years of age and had advanced dry AMD with an atrophic zone of at least 3 optic disc diameters and best corrected visual acuity of ≤20/400 in the worse-seeing study eye; no foveal light perception (absolute scotoma) but visual perception in the periphery, with preferred retinal locus determined by micro-perimetry; absence of photoreceptors and presence of the inner retina in the atrophic area as confirmed by optical coherence tomography (OCT); absence of choroidal neovascularization verified by retinal angiography. All other ocular and general pathologies that could contribute to the low visual acuity were excluded. Patients provided written informed consent to participate in the study.

Surgery

Surgical procedures were performed in the Fondation Ophtalmologique A. de Rothschild (Paris, France) under local or general anesthesia. The study eye was prepared for surgery with antiseptic solution. Complete 23-gauge vitrectomy and removal of the posterior hyaloid was performed. The macula was detached with a subretinal injection of BSS® via a 42-gauge needle inserted at a position away from the preferred retinal locus to avoid damage to the residual useful vision. A retinotomy (of approximately 2.5 mm) was performed at the margin of the atrophic area with vertical scissors and, if not totally detached by the BSS injection, the neural retina was dissected from the underlying atrophic pigment epithelium with a subretinal pick or spatula. A 2.4 mm sclerotomy was then created for intra-ocular implant delivery. The implant was inserted under the neural retina using silicone-coated forceps and placed near the target location under the retina. The implant was then guided to the desired central location by application of soft touch over the retina. Perfluorocarbon liquid was injected over the posterior pole to stabilize the implant and then removed via fluid-to-air exchange. Intraoperative OCT was used to verify retinal flattening, and the air was exchanged with a tamponade agent, either silicone oil or gas. In patients 1, 2 and 3, the air was exchanged with silicone oil (which was removed under local anesthesia one month later), and in patients 4 and 5, the air was exchanged with gas (hexafluoroethane and sulfur hexafluoride, respectively), and the 2.4 mm sclerotomy was closed.

After surgery, the patients were prescribed the usual postoperative topical treatment with a combination of dexamethasone and tobramycin eye drops 3 times a day for 4 weeks. Patients 4 and 5, who received an air-gas exchange, received 250 mg of acetazolamide 1 and 6 hours after surgery and placed in a prone position for 12 hours after surgery.

Assessment of prosthetic vision

The patients' rehabilitation and visual function assessment were carried out at the Clinical Investigation Center of Quinze-Vingts National Eye Hospital (Paris, France). To assess prosthetic vision independently of remaining natural vision, we made use of opaque video glasses with a Digital Mirror Display (DMD) in front of the operated eye (Figure 4). The projected images cover a field of 5.1 mm (17°) on the retina, with resolution of 10.5 μm. Maximum peak retinal irradiance was 3mW/mm^2, well within the thermal safety limits for chronic use of near-infrared light[30]. Brightness of the percept was controlled by pulse duration, of between 0.7 and 9.8 ms, in 0.7-ms steps. The glasses also included a miniature video camera, allowing patients to see a video stream of the visual scene captured by the camera (Figure 4). Alternatively, the system can project computer generated images into the eye. The camera captured a visual field of a 50 × 40 degrees, but only the central one-third of the image was projected onto the retina to match the 17° field of view of the display. Thus the angular magnification of the system was 1:1 – i.e. no optical or electronic zoom was used for acuity measurements or letter recognition.

Visual acuity was assessed using a computer-generated Landolt C in 4 different orientations (gap at the top, bottom, right or left), so that random response corresponds to 25% accuracy. The minimum optotype size was defined as the proper symbol recognition with at least 62.5% accuracy. To minimize the number of presentations, the study was conducted similarly to the Freiburg vision test[31].

For the letter recognition test, the alphabet was split into 3 groups of increasing difficulty, as applied previously in assessment of prosthetic vision[32]. Set A: L, T, E, F, J, H, I, U; Set B: A, Z, Q, V, N, W, O, C, D, M; Set C: K, R, G, X, B, Y, S, P. The overall methodology of the test (forced-choice, closed-set, with 4 repetitions of each letter) also matched the previous study[32], except that we used smaller letters of 2.8 cm at 30 cm distance.

Results

Following screening of the patient database at the Rothchild Foundation and Quinze-Vingts National Eye Hospital, those who met the inclusion criteria were invited to participate. The first patient was enrolled on November 13, 2017 and the last – on May 25, 2018. The 12-month examinations were completed on June 14, 2019.

Surgical Placement of Implant

Patient 1, operated under local anesthesia, moved when the implant was held by forceps under the retina, provoking inadvertent insertion of the chip into the choroid, accompanied by bleeding from the choroid that was partially evacuated during surgery. The blood resolved within 6 months, but an OCT image obtained at 6 months (Figure 2A) demonstrated that the chip was separated from the INL by a hyperreflective layer of approximately 70 μm in thickness. This layer could be a choroid and/or a scar tissue which formed above the chip in response to choroidal injury. For all other patients (2 – 5), surgery was performed under general anesthesia.

In two other cases, focal subretinal bleeding occurred from the retinal vessels at the retinotomy site, remaining at a distance from the implant and resolving within a few weeks. One patient with a gas exchange (#4) moved his head from the prone position immediately after surgery, before the retina had fully re-adhered. As a result, the chip shifted by remained in the scotoma (Figure 2B). The same patient did not take the prescribed medication (250 mg acetazolamide) after surgery, resulting in acute increase of intraocular pressure. This was successfully treated with intra-venous acetazolamide, followed by beta-blocker eyedrops for one week. In patients 2, 3 and 5, the implant remained stable, in a central location and in close proximity to the inner retina (Figure 3). The mean surgical time for all 5 implantations was 2h 4min, ranging from 1h 57min to 2h 10min.

Over the 12 months following surgery, the implants remained in the same location under the retina. To assess the effect of separation between electrodes and neurons on visual acuity and stimulation threshold, we measured the average distance between the chip and the bottom of the inner nuclear layer in each patient at 3-, 6- and 12-months post-op (Table 1). In patients with subretinal placement of the implant (#2–5), the average distance between the inner nuclear layer and implant was 35 to 39 μm at 12 months.

Natural Vision

Residual natural visual acuity in the treated eye did not decrease in any patient during the follow-up period (Table 1). In fact, it slightly improved in patients 1, 3, 4 and 5. This could be either due to neurotrophic benefit of the subretinal surgery or of the electrical stimulation[33], or a result of the vision rehabilitation training, which has the potential to improve preferred eccentric fixation.

Prosthetic Vision

In each patient, we first determined the perceptual threshold in terms of pulse duration, using a 16 pixels-wide circular spot at 10-Hz repetition rate, presented for up to 20 seconds at 3 mW/mm^2 irradiance (Table 1). Thresholds were determined with adaptive Best PEST procedure[34] of 15 to 20 repetitions. A strength-duration curve was also measured in each patient, from which the chronaxie and rheobase were computed. All patients described the percepts as bright white-yellow phosphenes inside their scotoma. At maximum pulse duration (9.8 ms), each patient described the percept as bright as a desk reading lamp. When we increased pulse frequency from 3 to 10 Hz, all patients reported that percepts were more persistent. Flickering further decreased when the frequency was increased to 30 Hz, and completely disappeared at 60 Hz. When tested in the dark, the patients could sometimes see the 880-nm radiation as a faint red light in the periphery. Therefore, during vision tests, all patients were asked about the color of percepts to ensure that only the white-yellow percepts were considered. Stimulation thresholds and perceptual brightness remained stable during the follow-up of the study.

In the visual field test (Octopus 900, Haag-Streit, Switzerland) at 6 and 12 months, all 5 patients reported light perception in the atrophic zone, elicited by the implant when the system was turned on, and no perception when the system was turned off. At 12 months test,

patient #5 also sometimes had a phantom visual perception not elicited by visual or electrical stimulation[35], when the device was turned off.

Tests with the computer-generated images defined the minimum width of a visible bar to be 1 pixel for patients #2–5, with the population average of identification 75+/−20% (p=0.002 and 95%CI of 59–87%), and 2 pixels for patient #1, with 90% identification (p=0.021 and 95%CI of 55–100%). In the forced-choice bar orientation test (vertical, horizontal, and 2 diagonals in opposing directions), patients 2, 3, 4 and 5 achieved 93.5+/− 3.8% accuracy. Patient 1, in whom the implant was placed in the choroid, identified the correct orientation with 28% accuracy, consistent with no improvement when using prosthetic vision (Table 1). Patients described the bars presented in various orientations as straight lines or elongated objects, demonstrating retinotopically correct perception.

The three patients with optimal placement of the implant (patients 2, 3 and 5) demonstrated visual acuity with Landolt C in the range of 20/460 – 20/550 (logMAR 1.37–1.44) within 12 months, which is 10 to 30% below the theoretical resolution limit (Nyquist sampling limit) for this pixel size (20/420, assuming 1° of the visual angle corresponds to 288 μm on the retina[36]). Patient #4 demonstrated prosthetic acuity of 20/800 (logMAR 1.6), while patient 1 could not resolve letters or optotypes of any size (Table 1). The population average prosthetic LogMAR acuity was 1.45 ± 0.10, with the 95% CI of (1.29, 1.62), calculated based on t distribution.

We asked patient 2 to recognize letters of 2.8 cm in height positioned 30 cm away from the face. This patient identified group A letters with 88% accuracy and 8 s median response time, group B letters with 80% accuracy and 7 s median response time, and group C letters with 75% accuracy and 11s median response time. Letter recognition did not involve the head scanning, but rather just the eye scanning of the image (see Supplemental video 1). This patient was able to read words, as illustrated in the same video. As a control, when the system was turned off, the patient had no visual perception since the opaque glasses used in these tests blocked the residual natural vision (see Supplemental video 2).

Discussion

The wireless nature of the PRIMA implant greatly simplifies the surgical procedures compared to the wired retinal prostheses - all the procedures in PRIMA surgery can be performed within two hours, as opposed to about 4 hours with Argus II[13] and 6–8 hours with Alpha IMS[19]. The most challenging part of the surgery is to separate the retina from RPE/choroid in atrophic macula, which often requires not only subretinal injection of fluid, but also careful delamination with a spatula. Implant release from the forceps in the intended location under the retina is also not trivial. To simplify this step in the procedure, we developed an injector of the implant, which will be used in the future trials. To avoid potential movement of patients in a wrong moment, as occurred with patient #1, we recommend performing the surgery under general anesthesia, if possible, or to ask patients to keep steady at critical moments. Patient compliance regarding the prone head position following the gas exchange procedure is essential, since otherwise the implant can shift from the original location prior to complete retinal reattachment, as was seen with patient #4.

Spatial resolution in patterned retinal stimulation depends not only on the pixel size, but also on the distance between electrodes and target neurons[37]. Ideally, for localized and efficient stimulation, it should not exceed the pixel radius. In patients 2–5, the distance between the INL and the implant is about 35–39 μm - smaller than the 50 μm radius of the current pixels (Table 1). However, in patient #1 it exceeds 100 μm, which might be the reason behind suboptimal performance of this subject.

From preclinical studies in rodents, we knew that many features of the retinal signal processing are preserved with subretinal prosthetics, such as flicker fusion at high frequencies[15,16], “on” and “off” responses with antagonistic center-surround[18], and non-linear summation of the inputs from bipolar cells into ganglion cells’ receptive fields[16]. However, we did not know what the actual human perception with such prosthesis will be. One of the most striking aspects of these clinical observations was that perception of prosthetic vision was remarkably “natural”: as soon as patients learned how to use video glasses, the prosthetic line patterns appeared in a correct shape right away, without scanning. Despite the likely indiscriminate electrical activation of multiple cell types in the inner retina (“on” and “off”, for example), our patients reported correct form perception of bright patterns (lines, letters, etc.) on a dark background. This may indicate that either the excitatory pathways dominate the perception, or that brain filters out conflicting inputs, and correctly interprets the images even when the signal encoding deviates from natural.

One reason for better and more consistent performance of the patients in the current trial compared to previous trials with a subretinal implant might be the patient selection: AMD patients may have much better-preserved inner retina in the relatively small central scotoma than at the end-stage RP, associated with a long-lasting and nearly complete loss of photoreceptors in the entire retina. Animal studies of the retinal remodeling in inherited retinal degeneration indicate that massive retinal reorganization occurs only when nearly all the photoreceptors are gone[22,38] – a situation that does not occur in AMD patients.

In summary, within the limits of a small study, we have demonstrated that sub macular implantation of a wireless photovoltaic array in patients with geographic atrophy is feasible, the implant is stable over time, and it did not decrease the eccentric natural acuity. All 4 patients with subretinal placement of the chip achieved letter acuity. In 3 patients with central chip placement, prosthetic acuity was only 10 to 30% below the sampling limit for the current pixel size. The use of optical or electronic magnification in the future glasses or implants with smaller pixels may further improve the prosthetic visual acuity. As the next step, we will test the transparent (augmented reality) glasses to allow simultaneous use of the prosthetic central and natural peripheral vision, which should improve the benefit of the PRIMA system in daily living.

Supplementary Material

Refer to Web version on PubMed Central for supplementary material.

Acknowledgements

Authors would like to thank first the patients who participated in the study. Second, authors would like to express their gratitude to the Pixium Vision team who designed, fabricated and tested the PRIMA system. We are also grateful to the Scientific and Medical Advisory Board of the company for their guidance on the clinical trial design. Authors would also like to acknowledge all the scientific, R&D, medical and clinical research staff who continue the patients care, rehabilitation and evaluation.

Financial support:

The study was funded by Pixium Vision and in part by the Sight Again project under the Structural R&D Projects for Competitiveness (PSPC) and Investment for the Future (PIA) funding, managed by Bpifrance. D.P.'s funding was provided in part by the National Institutes Health (grant R01-EY027786). Biomedical Research Centre at Moorfields Eye Hospital is acknowledged and supported in part by the National Institute for Health Research, UK. Clinical Investigation Center at the Quinze-Vingts National Hospital is supported in part by the Inserm-DHOS, France.

References

1. Wong WL, Su X, Li X, et al. Global prevalence of age-related macular degeneration and disease burden projection for 2020 and 2040: a systematic review and meta-analysis. Lancet Glob Health 2014;2:e106–16. [PubMed: 25104651]
2. Friedman DS, Tomany SC, McCarty C, De Jong P. Prevalence of age-related macular degeneration in the United States. Arch ophthalmol 2004;122:564–72. [PubMed: 15078675]
3. Mazzoni F, Novelli E, Strettoi E. Retinal ganglion cells survive and maintain normal dendritic morphology in a mouse model of inherited photoreceptor degeneration. J Neurosci 2008;28:14282–92. [PubMed: 19109509]
4. Humayun MS, Prince M, de Juan E, et al. Morphometric analysis of the extramacular retina from postmortem eyes with retinitis pigmentosa. Invest Ophth Vis Sci 1999;40:143–8.
5. Kim SY, Sadda S, Pearlman J, et al. Morphometric analysis of the macula in eyes with disciform age-related macular degeneration. Retina 2002;22:471–7. [PubMed: 12172115]
6. Zrenner E Fighting blindness with microelectronics. Sci Transl Med 2013;5:210ps16.
7. Zrenner E, Bartz-Schmidt KU, Benav H, et al. Subretinal electronic chips allow blind patients to read letters and combine them to words. Proc Biol Sci 2011;278:1489–97. [PubMed: 21047851]
8. Mathieson K, Loudin J, Goetz G, et al. Photovoltaic Retinal Prosthesis with High Pixel Density. Nat Photonics 2012;6:391–7. [PubMed: 23049619]
9. Behrend MR, Ahuja AK, Humayun MS, Chow RH, Weiland JD. Resolution of the epiretinal prosthesis is not limited by electrode size. IEEE Trans Neural Syst Rehabil Eng 2011;19:436–42. [PubMed: 21511569]
10. Jensen RJ, Rizzo JF 3rd. Thresholds for activation of rabbit retinal ganglion cells with a subretinal electrode. Exp Eye Res 2006;83:367–73. [PubMed: 16616739]
11. Luo YH-L, da Cruz L. The Argus® II retinal prosthesis system. Progress in retinal and eye research 2016;50:89–107. [PubMed: 26404104]
12. Ahuja AK, Yeoh J, Dorn JD, et al. Factors Affecting Perceptual Threshold in Argus II Retinal Prosthesis Subjects. Transl Vis Sci Technol 2013;2:1.
13. Humayun MS, Dorn JD, da Cruz L, et al. Interim results from the international trial of Second Sight's visual prosthesis. Ophthalmology 2012;119:779–88. [PubMed: 22244176]
14. Nanduri D, Fine I, Horsager A, et al. Frequency and Amplitude Modulation Have Different Effects on the Percepts Elicited by Retinal Stimulation. Invest Ophth Vis Sci 2012;53:205–14.
15. Lorach H, Goetz G, Mandel Y, et al. Performance of photovoltaic arrays in-vivo and characteristics of prosthetic vision in animals with retinal degeneration. Vision Res 2015;111:142–8. [PubMed: 25255990]
16. Lorach H, Goetz G, Smith R, et al. Photovoltaic restoration of sight with high visual acuity. Nature Medicine 2015;21:476–82.

17. Stingl K, Bartz-Schmidt KU, Gekeler F, Kusnyerik A, Sachs H, Zrenner E. Functional outcome in subretinal electronic implants depends on foveal eccentricity. Invest Ophthalmol Vis Sci 2013;54:7658–65. [PubMed: 24150759]
18. Ho E, Smith R, Goetz G, et al. Spatiotemporal characteristics of retinal response to network-mediated photovoltaic stimulation. J Neurophysiol 2017;119:389–400. [PubMed: 29046428]
19. Stingl K, Bartz-Schmidt KU, Besch D, et al. Subretinal Visual Implant Alpha IMS--Clinical trial interim report. Vision Res 2015;111:149–60. [PubMed: 25812924]
20. Stingl K, Schippert R, Bartz-Schmidt KU, et al. Interim Results of a Multicenter Trial with the New Electronic Subretinal Implant Alpha AMS in 15 Patients Blind from Inherited Retinal Degenerations. Front Neurosci 2017;11:445. [PubMed: 28878616]
21. Loudin JD, Simanovskii DM, Vijayraghavan K, et al. Optoelectronic retinal prosthesis: system design and performance. Journal of Neural Engineering 2007;4:S72–S84. [PubMed: 17325419]
22. Marc RE, Jones BW. Retinal remodeling in inherited photoreceptor degenerations. Mol Neurobiol 2003;28:139–47. [PubMed: 14576452]
23. Mathieson K, Loudin J, Goetz G, et al. Photovoltaic retinal prosthesis with high pixel density. Nature Photonics 2012;6:391–7. [PubMed: 23049619]
24. Goetz GA, Mandel Y, Manivanh R, Palanker DV, Cizmar T. Holographic display system for restoration of sight to the blind. Journal of Neural Engineering 2013;10.
25. Ho E, Smith R, Goetz G, et al. Spatiotemporal characteristics of retinal response to network-mediated photovoltaic stimulation. J Neurophysiol 2018;119:389–400. [PubMed: 29046428]
26. Ho E, Lorach H, Goetz G, et al. Temporal structure in spiking patterns of ganglion cells defines perceptual thresholds in rodents with subretinal prosthesis. Sci Rep-Uk 2018;8:3145.
27. Boinagrov D, Lei X, Goetz G, et al. Photovoltaic Pixels for Neural Stimulation: Circuit Models and Performance. IEEE Trans Biomed Circuits Syst 2016;10:85–97. [PubMed: 25622325]
28. Ho E, Lei X, Flores T, et al. Characteristics of prosthetic vision in rats with subretinal flat and pillar electrode arrays. J Neural Eng 2019;16:066027. [PubMed: 31341094]
29. Prévot P-H, Gehere K, Arcizet F, et al. Behavioural responses to a photovoltaic subretinal prosthesis implanted in non-human primates. Nature Biomedical Engineering 2019.
30. Lorach H, Wang J, Lee DY, Dalal R, Huie P, Palanker D. Retinal safety of near infrared radiation in photovoltaic restoration of sight. Biomed Opt Express 2016;7:13–21. [PubMed: 26819813]
31. Bach M The Freiburg Visual Acuity test - Automatic measurement of visual acuity. Optometry and Vision Science 1996;73:49–53. [PubMed: 8867682]
32. da Cruz L, Coley BF, Dorn J, et al. The Argus II epiretinal prosthesis system allows letter and word reading and long-term function in patients with profound vision loss. Br J Ophthalmol 2013;97:632–6. [PubMed: 23426738]
33. Castaldi E, Cicchini GM, Cinelli L, Biagi L, Rizzo S, Morrone MC. Visual BOLD Response in Late Blind Subjects with Argus II Retinal Prosthesis. PLoS Biol 2016;14:e1002569. [PubMed: 27780207]
34. Lieberman HR, Pentland AP. Microcomputer-Based Estimation of Psychophysical Thresholds - the Best Pest. Behav Res Meth Instr 1982;14:21–5.
35. Pearson J, Westbrook F. Phantom perception: voluntary and involuntary nonretinal vision. Trends Cogn Sci 2015;19:278–84. [PubMed: 25863415]
36. Drasdo N, Fowler CW. Non-linear projection of the retinal image in a wide-angle schematic eye. Br J Ophthalmol 1974;58:709–14. [PubMed: 4433482]
37. Palanker D, Vankov A, Huie P, Baccus S. Design of a High Resolution Optoelectronic Retinal Prosthesis. Journal of Neural Engineering 2005;2:S105–20. [PubMed: 15876646]
38. Marc R, Jones B, Anderson J, et al. Neural Reprogramming in Retinal Degeneration. Invest Ophth Vis Sci 2007;48:3364–71.

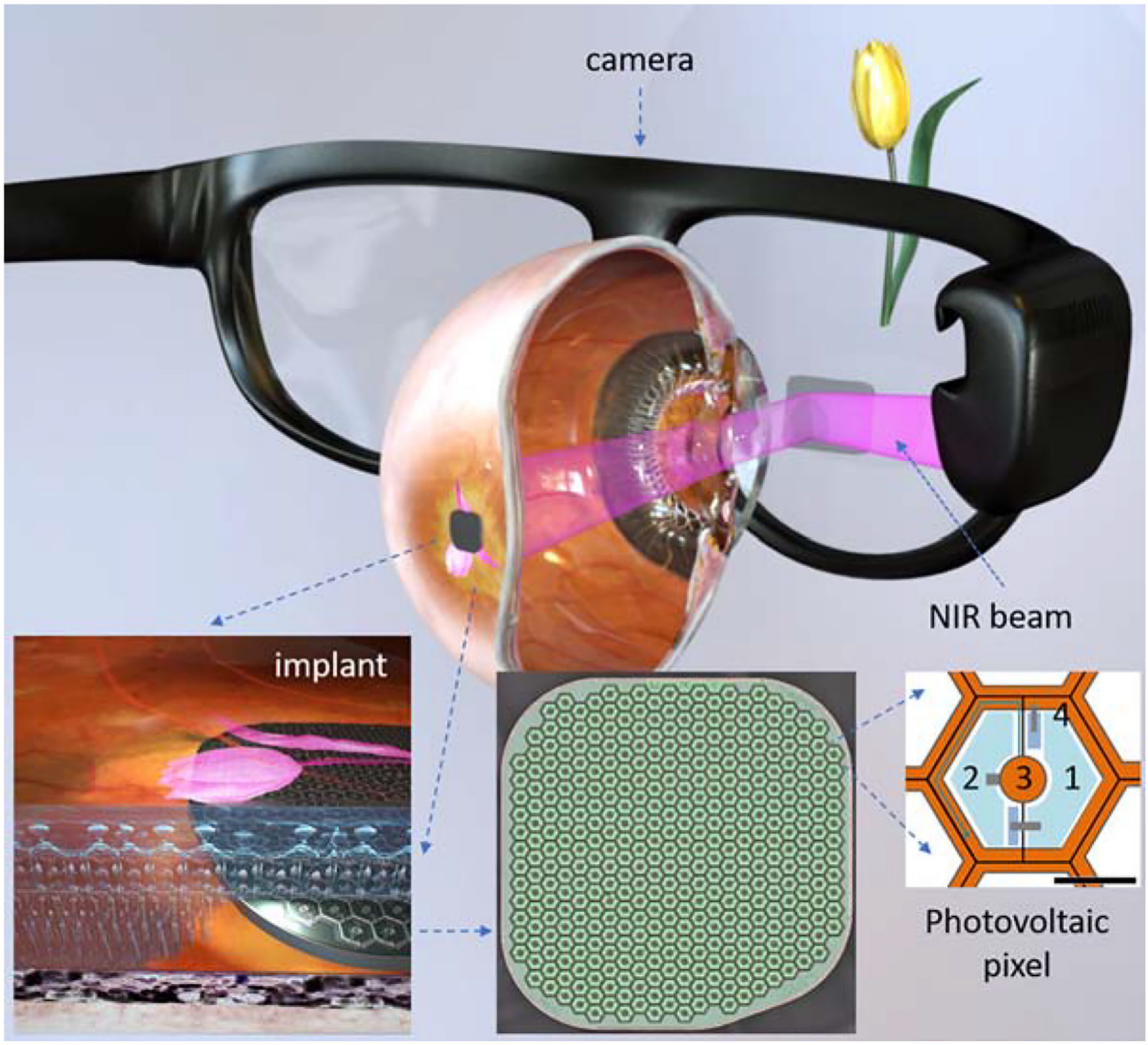

Figure 1.

System diagram of the photovoltaic retinal prosthesis, including camera integrated into augmented reality-like video glasses, with the processed image projected onto the retina using pulsed NIR light. Subretinal wireless photovoltaic array converts pulsed light into pulsed electric current in each pixel to stimulate the adjacent inner retinal neurons. Each pixel includes two diodes (1 and 2), connected in series between the active (3) and return (4) electrodes. Scale bar is 50 μm.

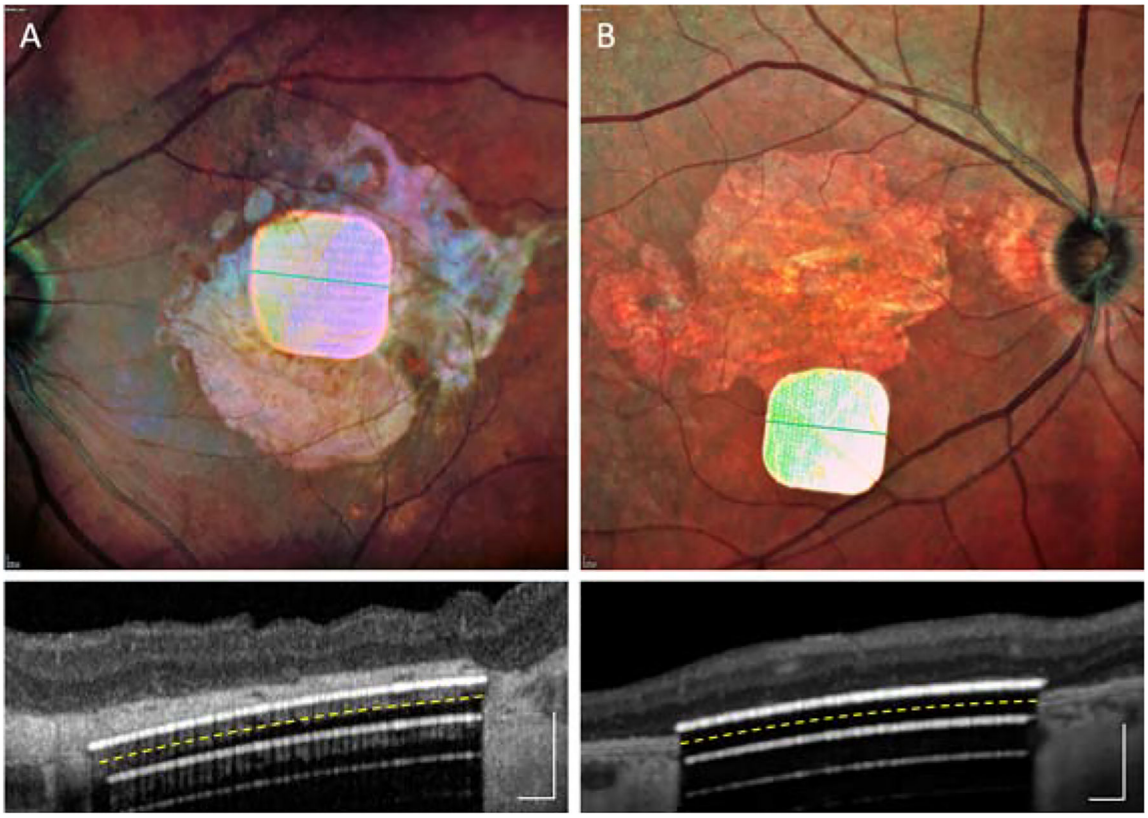

Figure 2.

Fundus photos and OCTs taken along the green line, with two implants in unintended locations: (A) in the choroid in patient #1; (B) in the periphery of the macula in patient #4. Scale bars are 200 μm. Yellow dash line indicates the back side of the implant. White lines underneath the implant are the OCT reflections. Images obtained during the 6-weeks to 6-months post-op visits.

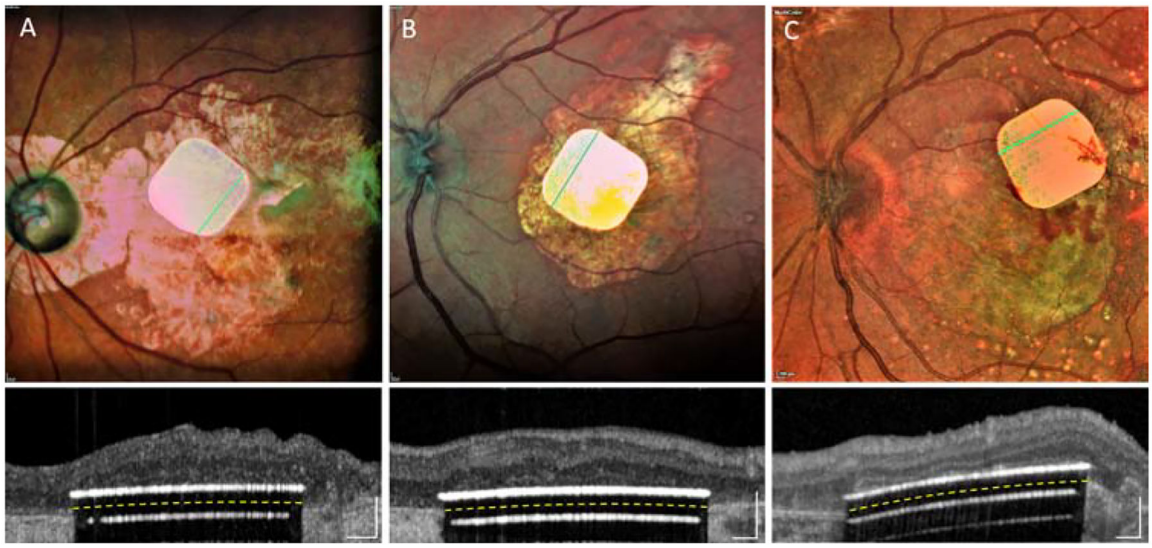

Figure 3.
Fundus photos and OCTs with three implants in intended locations: (A) patient #2; (B) patient #3; (C) patient #5. Images obtained during the 6-weeks to 6-months post-op visits.

Figure 4.

A) Opaque video glasses with an integrated camera (white arrow) used in the feasibility study. B) Letter recognition and reading tests with one of the subjects, using the camera mode.

Table 1.

Residual natural vision, anatomical and functional outcomes with the implant.

Test \ Patient	1	2	3	4	5
Residual peripheral vision					
Pre-op eccentric natural acuity in the study eye	20/400 LogMAR 1.3	20/800 LogMAR 1.6	20/1000 LogMAR 1.7	20/500 LogMAR 1.4	20/500 LogMAR 1.4
Post-op eccentric natural acuity in the study eye (12 months)	20/320 LogMAR 1.2	20/800 LogMAR 1.6	20/800 LogMAR 1.6	20/400 LogMAR 1.3	20/400 LogMAR 1.3
Implant location					
Implant location in the macula	Intra-choroidal	Central subretinal	Central subretinal	Off-center subretinal	Central subretinal
Average distance from implant to bottom of INL at 3, 6, 12 months (μm)	127	34	43	37	51
	103	28	35	38	39
	138	39	39	35	37
Perceptual stimulation thresholds					
Chronaxie (ms)	NA	2.5	2.3	2.2	2.1
Rheobase (mW/mm^2)	NA	1.0	0.4	1.4	0.5
Threshold pulse duration (ms) for $3mW/mm^2$	2.1	0.8	0.7	1.0	0.8
Central vision					
Natural central visual perception	None	None	None	None	None
Prosthetic bar orientation, % correct, [95% CI], %	28 [20–40]	96 [93–98]	96 [93–98]	94 [86–98]	88 [75–95]
Prosthetic min. bar width on retina, pix, (% correct) [95% CI], %	2 (90%) [55–100]	1 (100%) [69–100]	1 (70%) [35–93]	1 (50%) [19–82]	1 (80%) [44–97]
Prosthetic central acuity Min. Landolt C gap, pix	Light perception	20/550 LogMAR 1.44 1.3 pix	20/500 LogMAR 1.4 1.2 pix	20/800 LogMAR 1.6 1.9 pix	20/460 LogMAR 1.37 1.1 pix